Biphenyl Containing Amido Schiff base Derivative as a Turn-on Fluorescent Chemosensor for Al^{3+} and Zn^{2+} ions

Anamika Hoque,[a] Md. Sanaul Islam,[a] Mehebub Ali Khan,[a] Soumen Ghosh[a]*, Md. Asraful Sekh[b]*, Sahid Hussain[c]* and Md. Akhtarul Alam[a]*

[a]Department of Chemistry, Aliah University, Action Area IIA/27, New Town, Kolkata-700160, India

[b]Department of Electronics and Communication Engineering, Aliah University, Action Area IIA/27, New Town, Kolkata-700160, India

[c]Department of Chemistry, Indian Institute of Technology, Patna 801106, India

*Corresponding author, E-mail: soumen0003@gmail.com (S.G), asekh@yahoo.com (M.A.S.), sahid@iitp.ac.in (S.H) and alam_iitg@yahoo.com (M.A.A.)

Table of Contents

1. General

1.1. Materials

All reagents and spectroscopic grade solvents were used as received from commercial sources without further purification. All cations in the form of perchlorate / nitrate salts were purchased from Sigma-Aldrich Chemical Company. Solvents used for spectroscopic studies were of spectroscopic grade. Aqueous medium experiments have been done in deionized water.

1.2. Methods

Hitachi UV–vis (Model U-3501) spectrophotometer and Perkin Elmer LS-55 spectro fluorometer, were used to record the absorption spectra and emission spectra respectively. IR spectra (KBr pellet, 4000–400 cm^{-1}) were recorded on a Parkin Elmer model 883 infrared spectrophotometer. Shimadzu LCMS-2020 was used for recording mass spectrum. ^{1}H NMR and ^{13}C NMR spectra were recorded on a Bruker, Avance 500 spectrometer, where chemical shifts (δ in ppm) were determined with respect to tetramethylsilane (TMS) as internal standards.

2. Benesi-Hildebrand Plot:

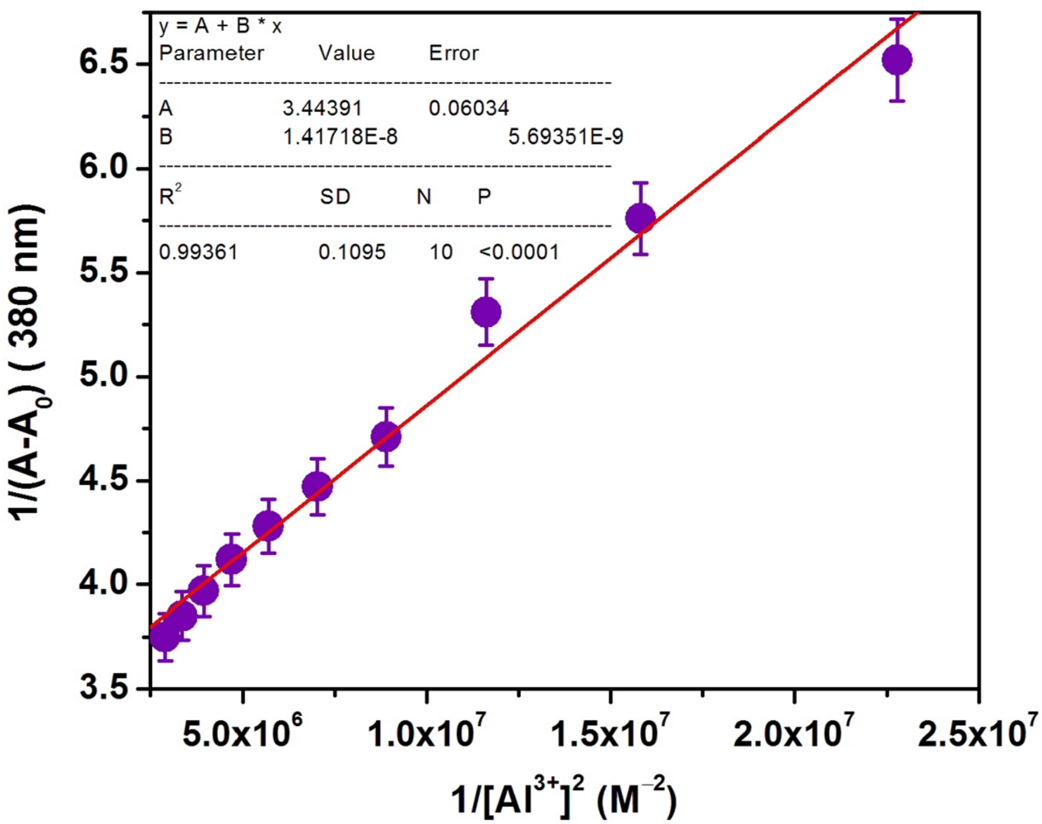

Figure S1. B–H plot for UV-vis titration of **1** with Al^{3+}

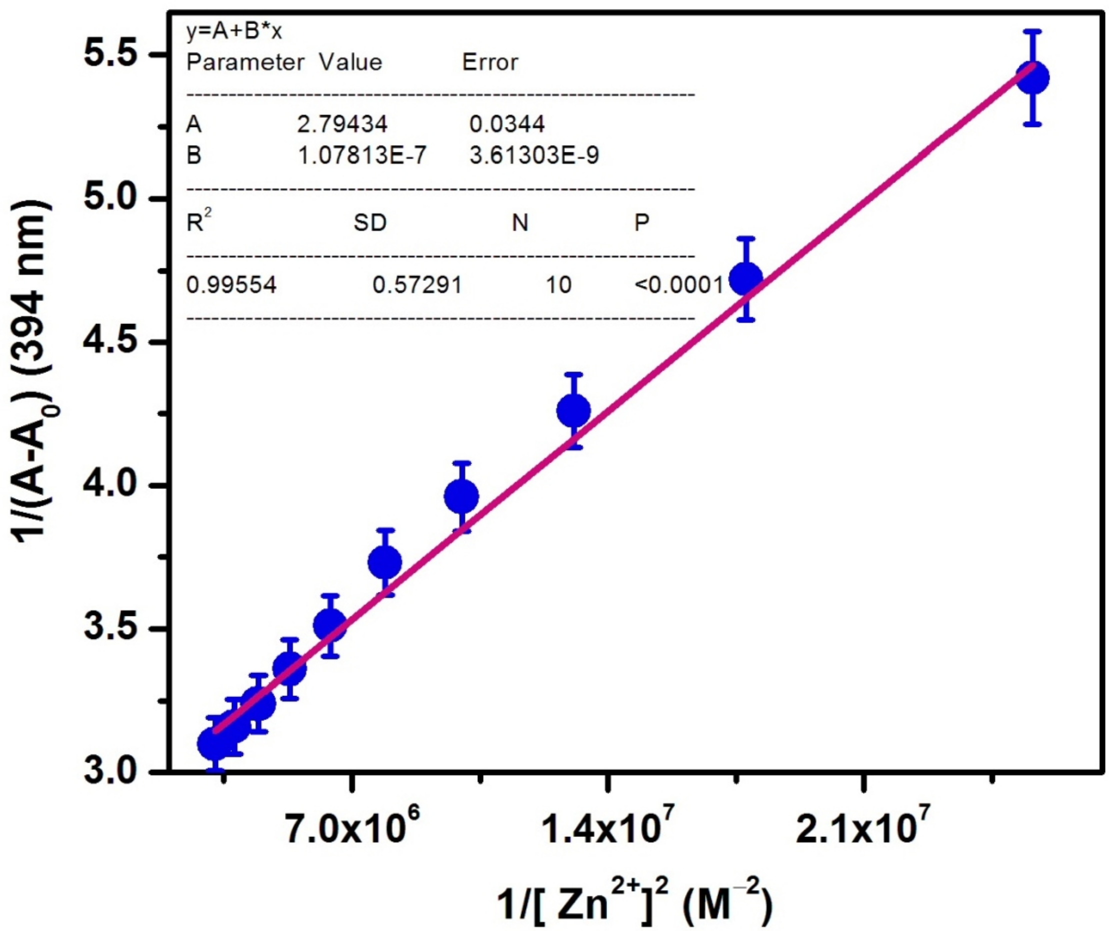

Figure S2. B–H plot for UV-vis titration of **1** with Zn^{2+}.

3. UV-vis titration:

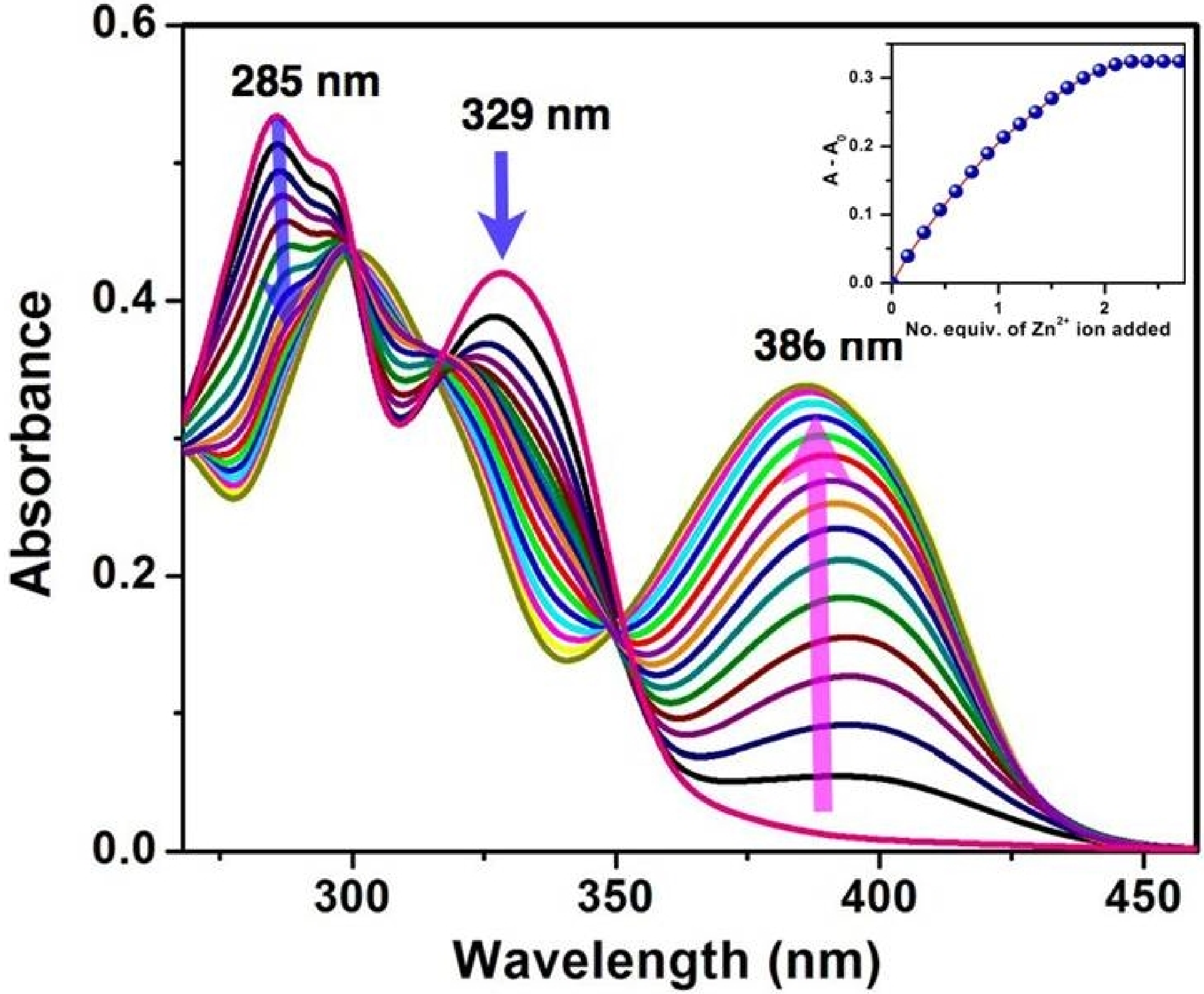

Figure S3. UV-vis titration of **1** (1×10^{-5} M) in DMF- H_2O solvent (v/v, 7:3) upon addition of (0-3 equivalents) of Zn^{2+} ion (inset: absorbance at 386 nm as a function of the equivalence of Zn^{2+} ion).

4. Job's plot:

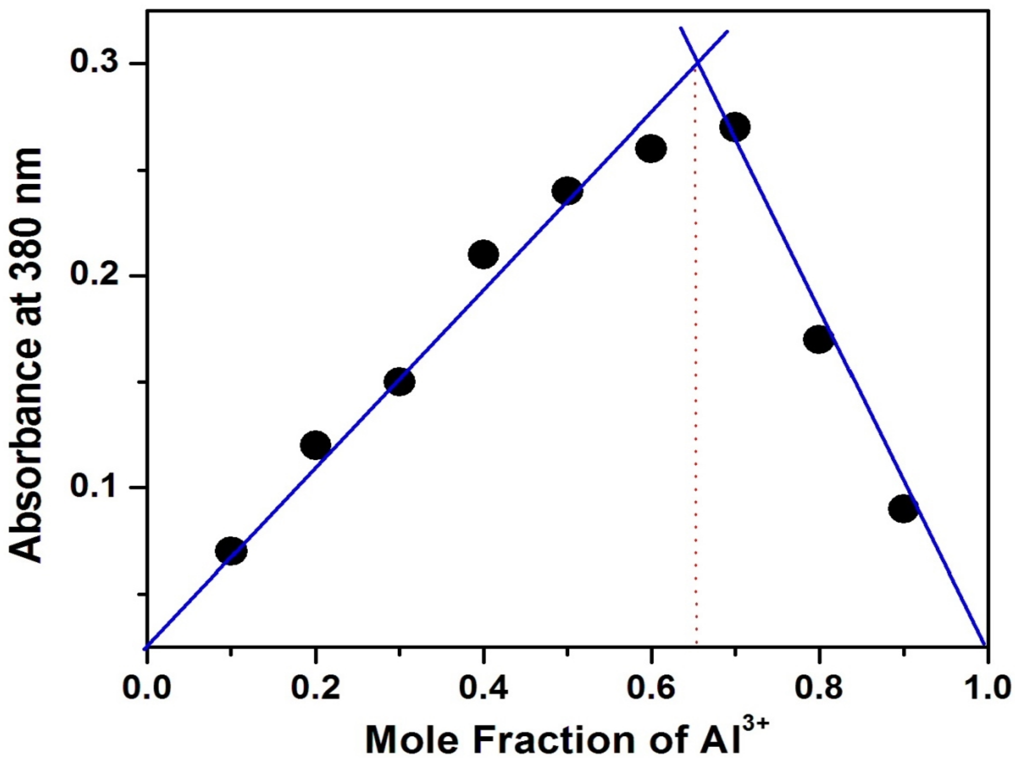

Figure S4. Job's plot for determining the stoichiometry of sensor **1** and Al^{3+} in the complex.

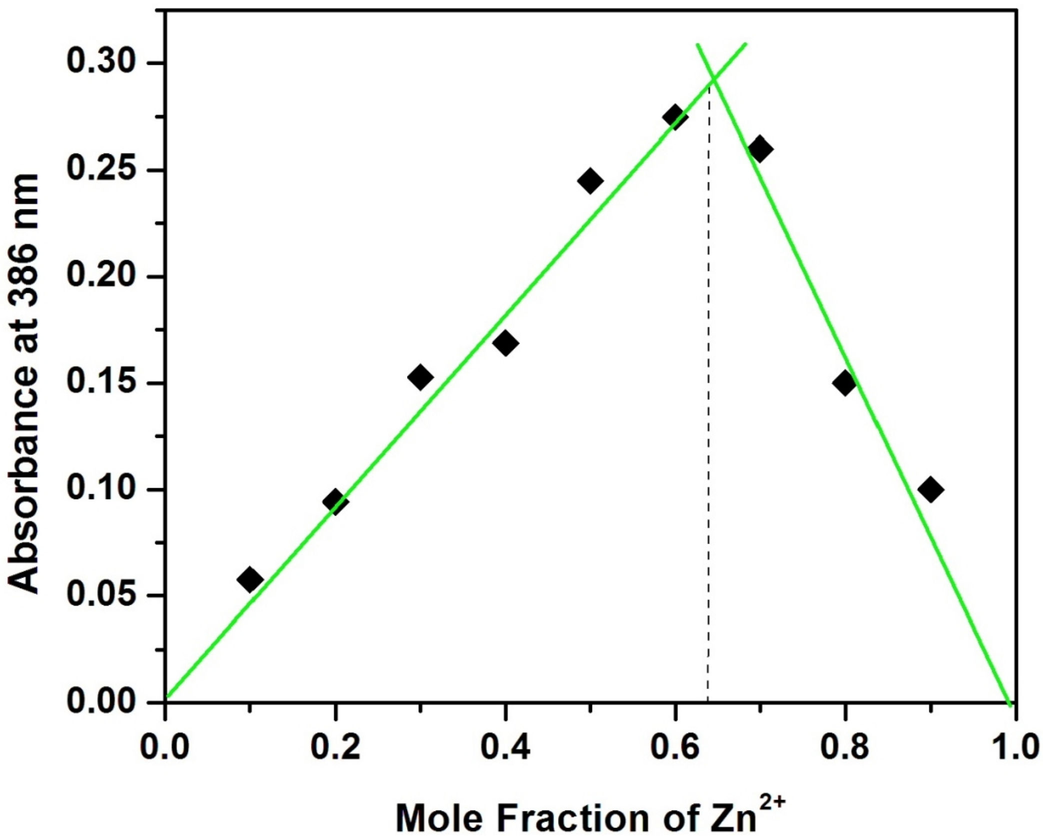

Figure S5. Job's plot for determining the stoichiometry of molecule **1** and Zn^{2+} in the complex.

5 . Fluorescence spectra

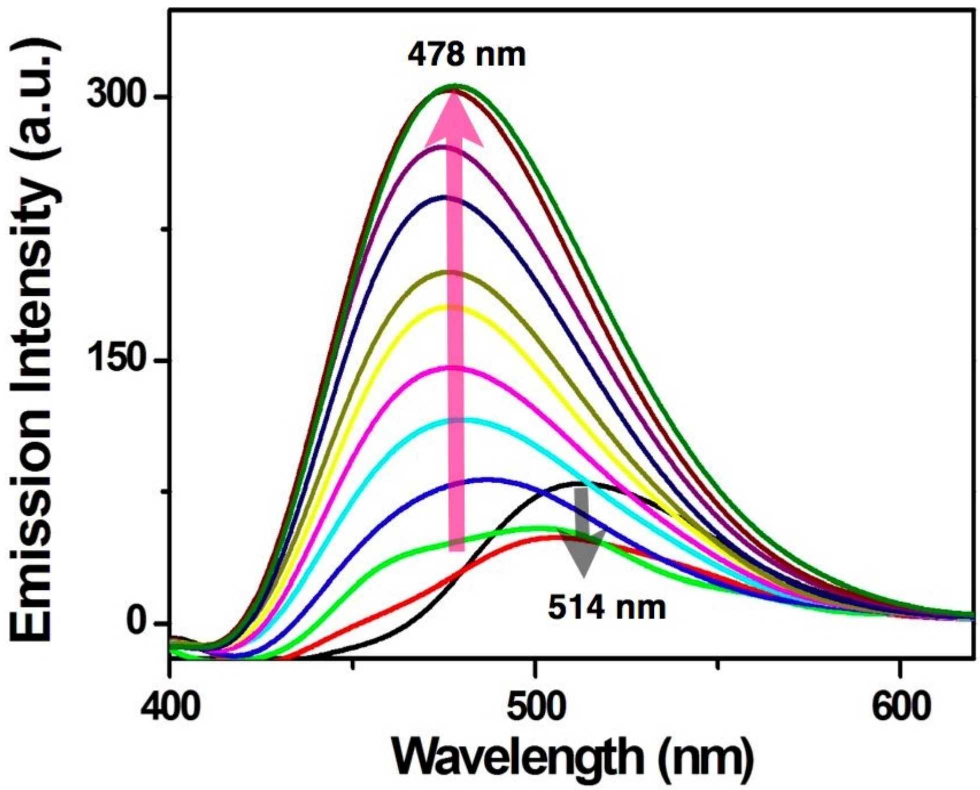

Figure S6. Changes in fluorescence spectra of sensor **1** (1×10^{-6} M) in the DMF-H_2O solution (v/v, 7:3) induced by Zn^{2+} ion.

6. Detection limit:

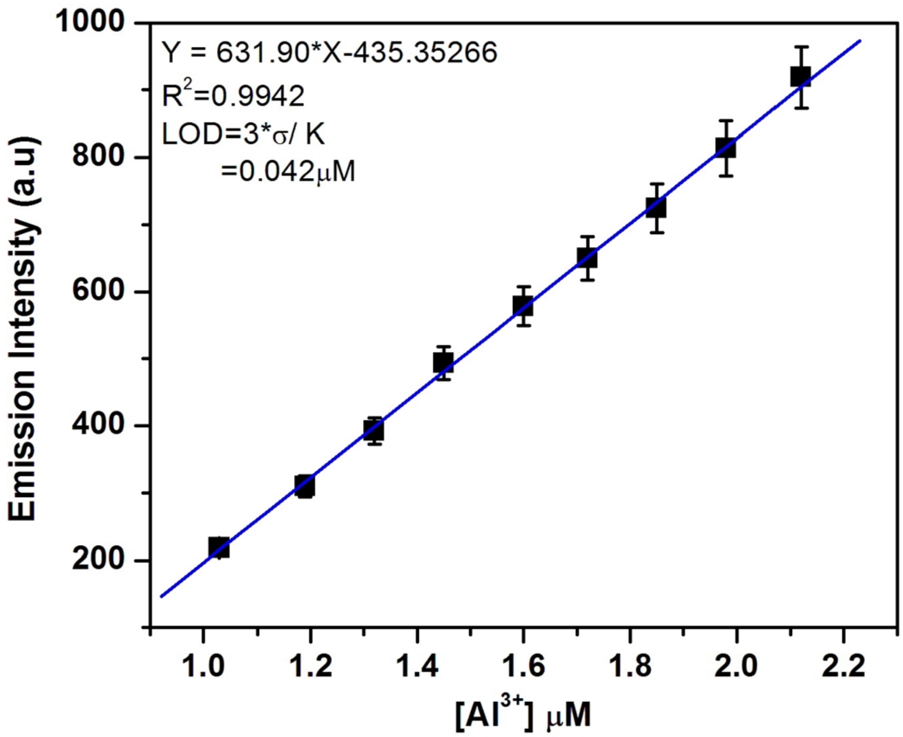

Figure S7. Detection limit of molecule **1** to Al^{3+} based on 3σ/slope

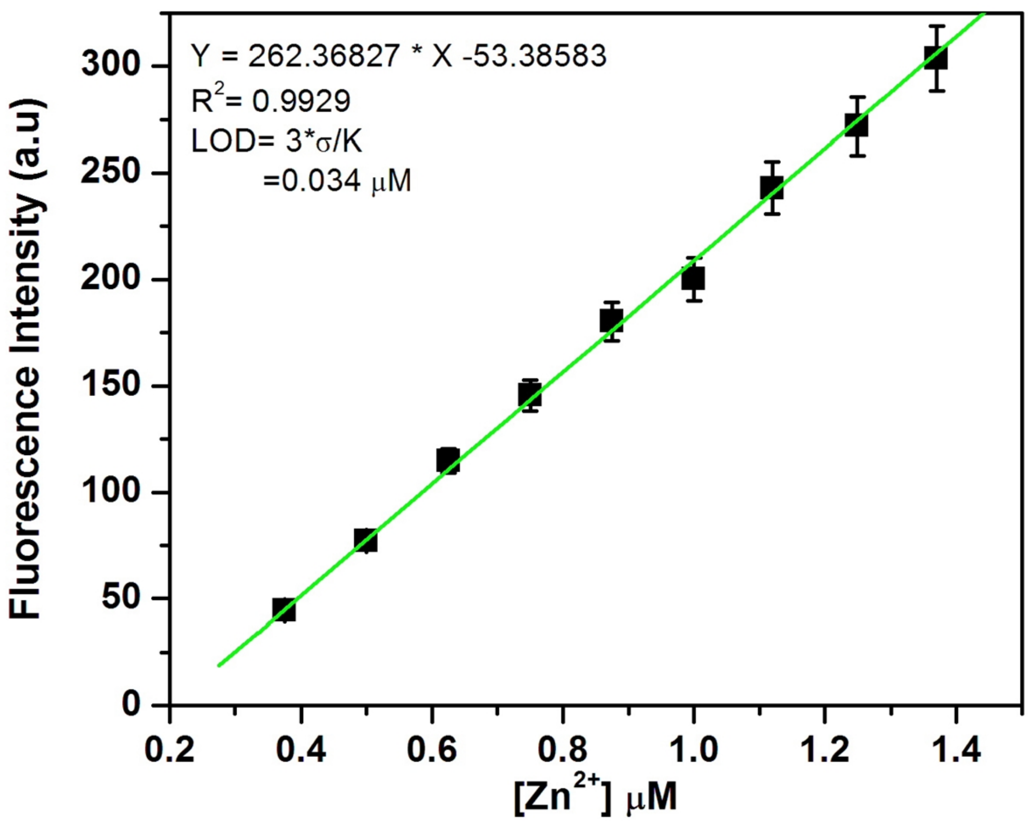

Figure S8. Detection limit of molecule **1** to Zn^{2+} based on 3σ/slope.

7. ^{1}H NMR titration spectra:

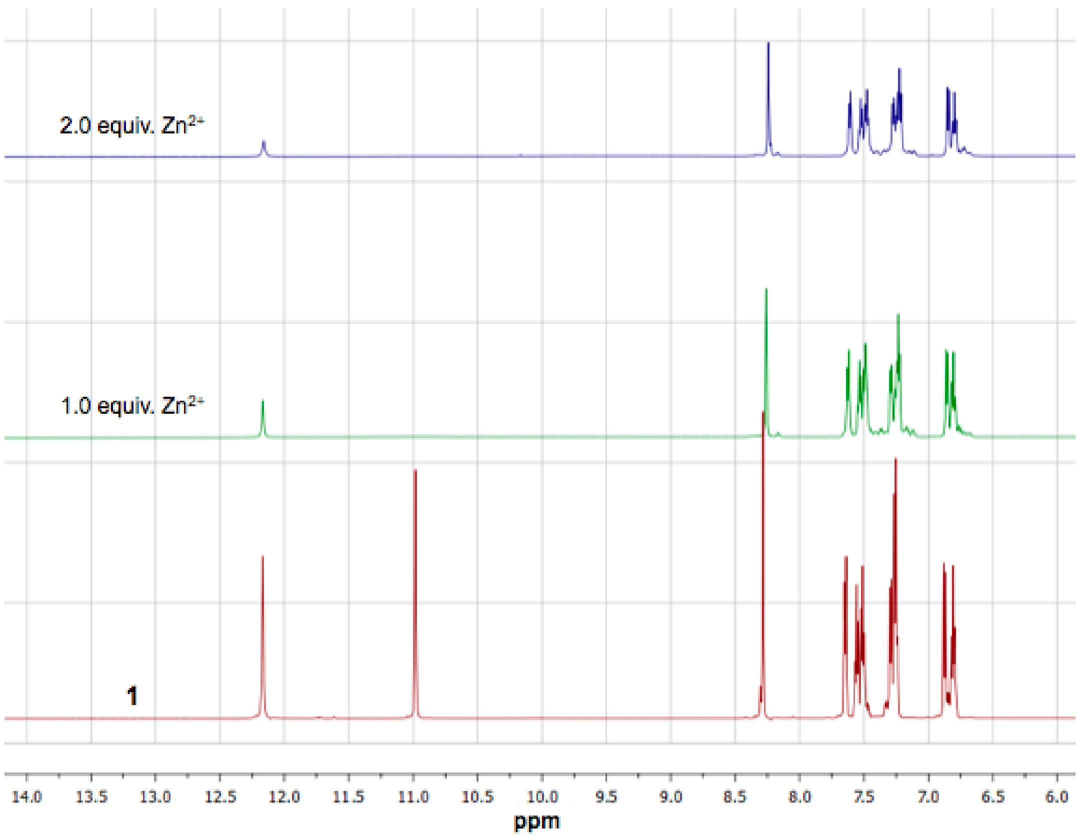

Figure S9. Partial ^{1}H NMR titration spectra of sensor **1** in d_6-DMSO upon addition of different amount of Zn^{2+} ion

8. Mass spectra:

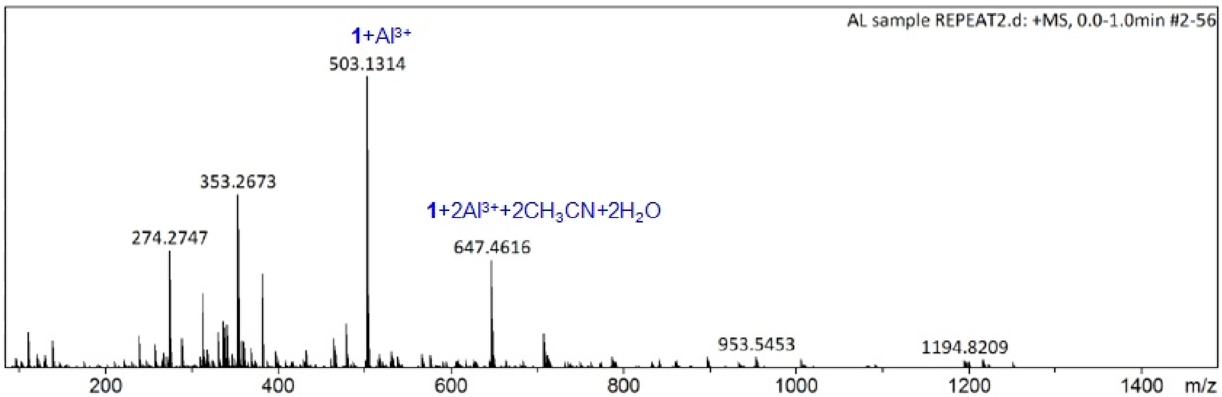

Figure S10. Mass spectrum of **1**-Al^{3+} complex.

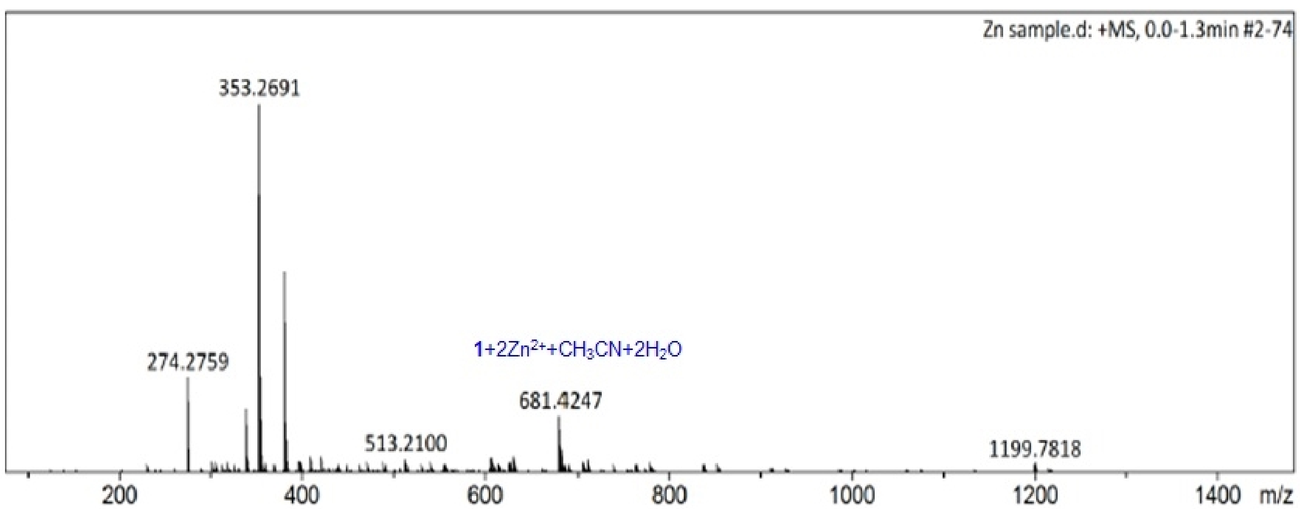

Figure S11. Mass spectrum of **1**-Zn^{2+} complex.

9. Probable structure:

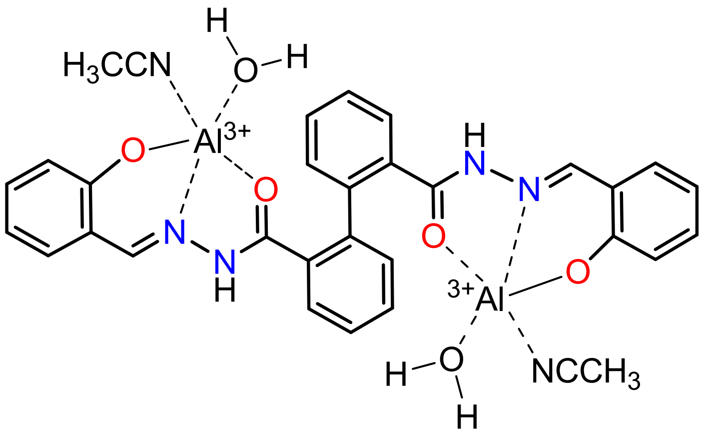

Figure S12. Probable structure of **1**- Al^{3+} complex

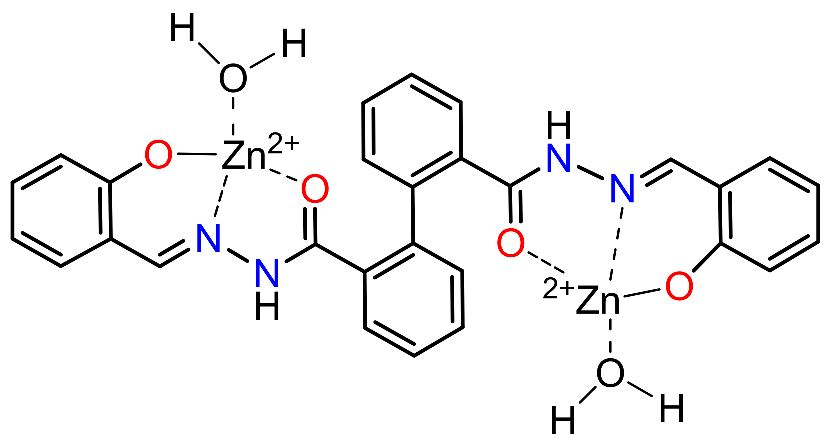

Figure S13. Probable structure of **1**- Zn^{2+} complex

10. Effect of pH

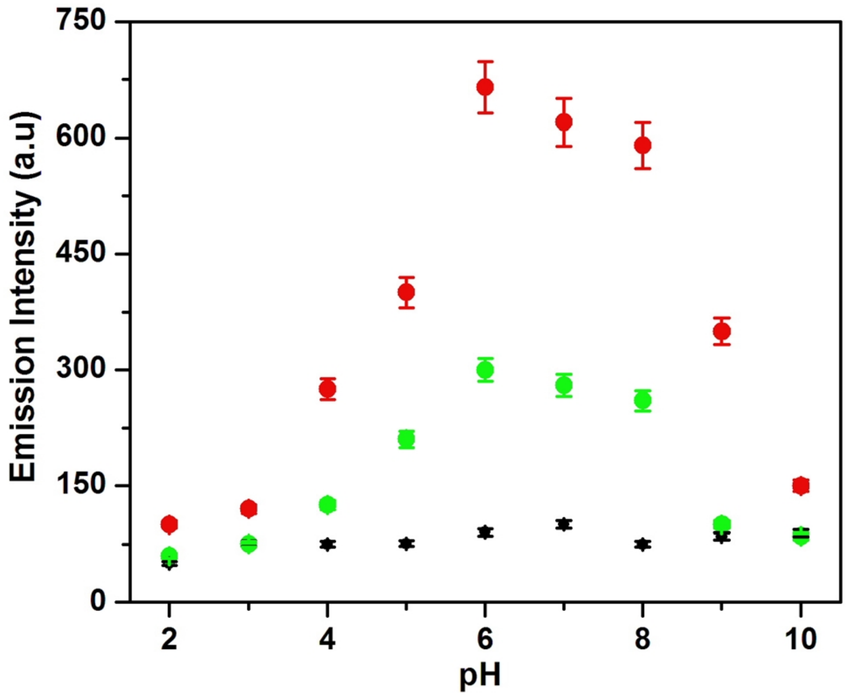

Figure S14. Change in fluorescence intensity sensor **1** (1×10^{-6} M) (●), its Al^{3+} (●) and Zn^{2+} (●) complexes in different pH values.

11. Competition experiment:

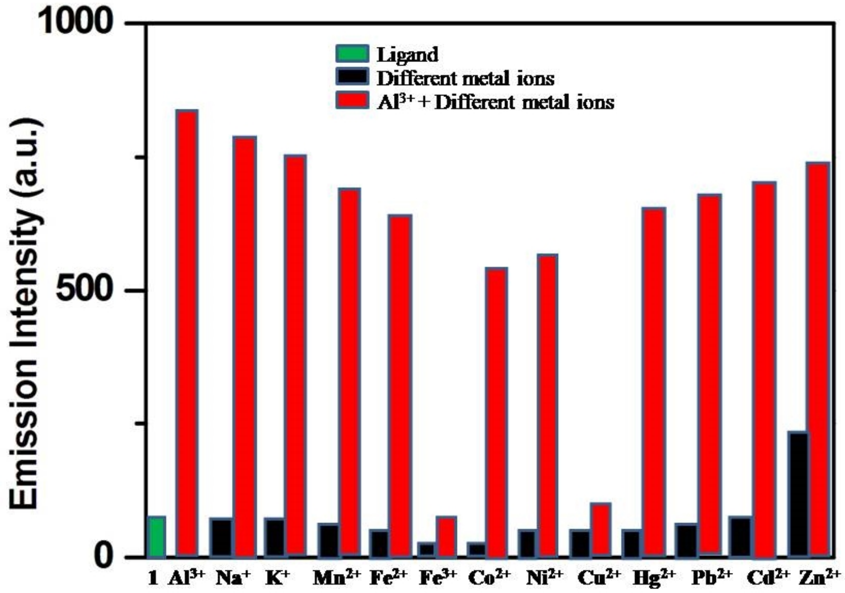

Figure S15 Competition experiments of **1**, a plot of fluorescence intensity at 458 nm of **1** with addition of 3.0 equiv. of Al^{3+}, and then 10.0 equiv. of various metal ions, (λex: 350 nm).

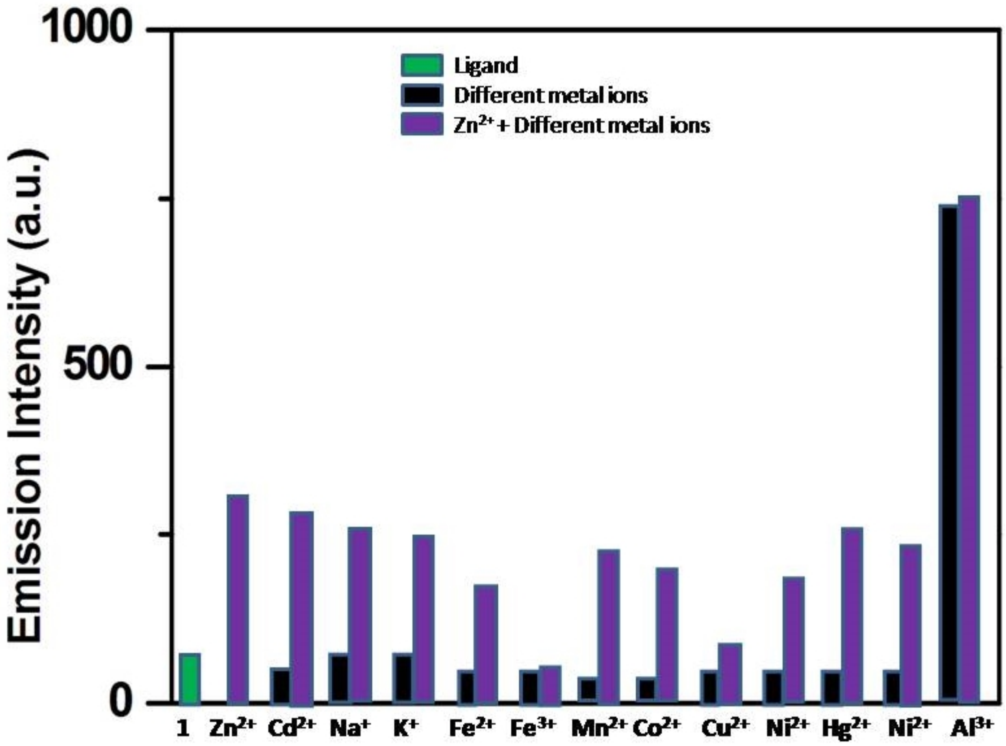

Figure S16. Competition experiments of **1**, a plot of fluorescence intensity at 478 nm of **1** with addition of 3.0 equiv. of Zn^{2+}, and then 10.0 equiv. of various metal ions, (λ_{ex}: 350 nm).

12. UV-Vis spectra with EDTA:

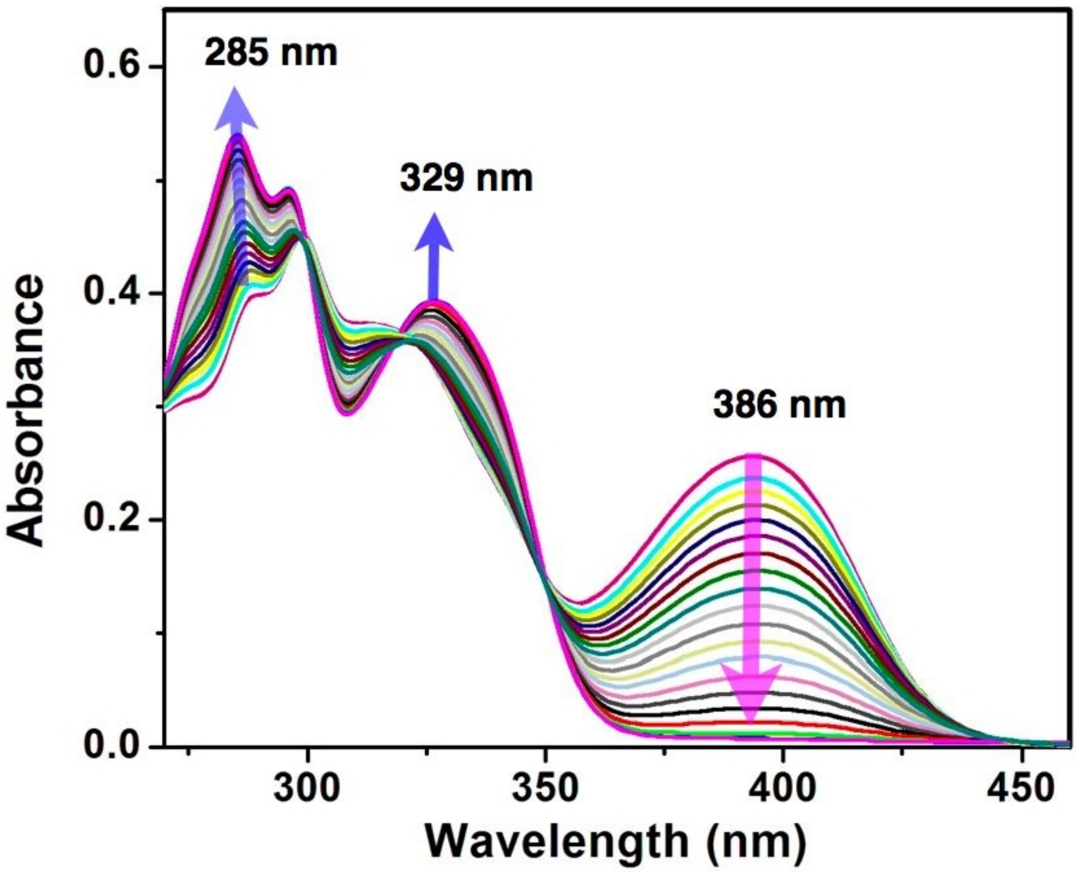

Figure S17. UV-Vis titration of **1**- Zn^{2+} complex with EDTA in DMF- H_2O solvent (v/v, 7:3).

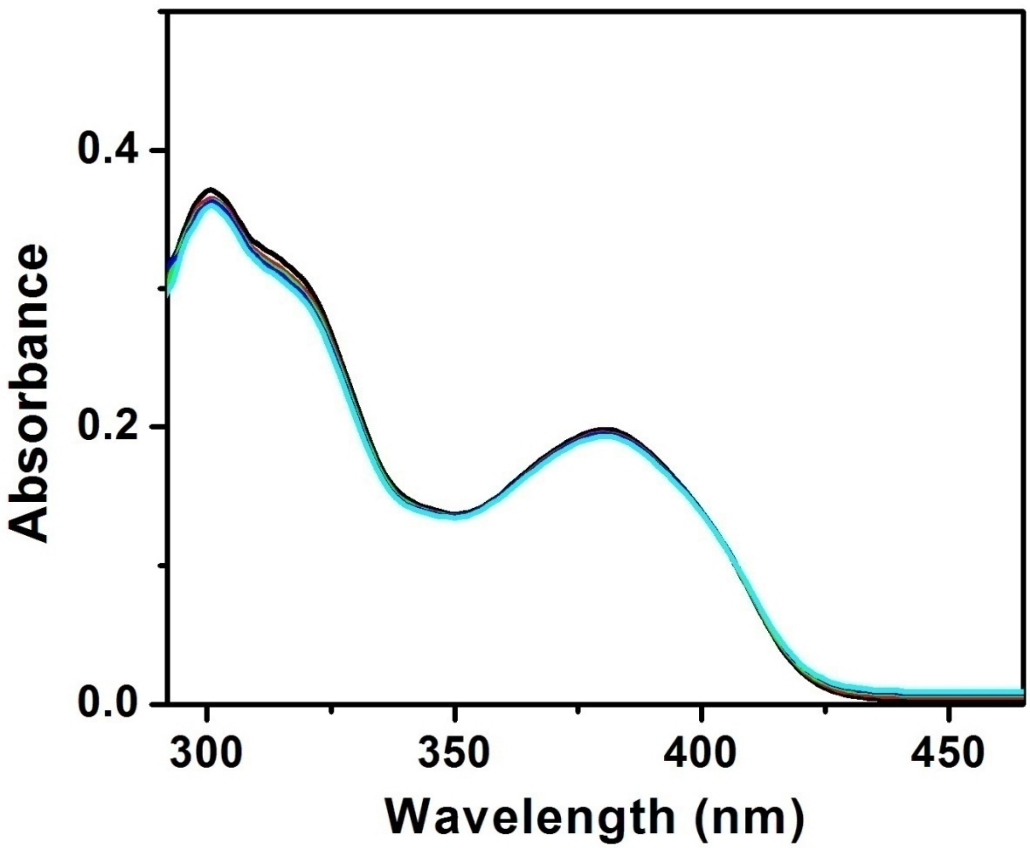

Figure S18. UV-Vis titration of Al^{3+}-**1** complex with EDTA in DMF- H_2O solvent (v/v, 7:3).

13. Emission spectra with EDTA:

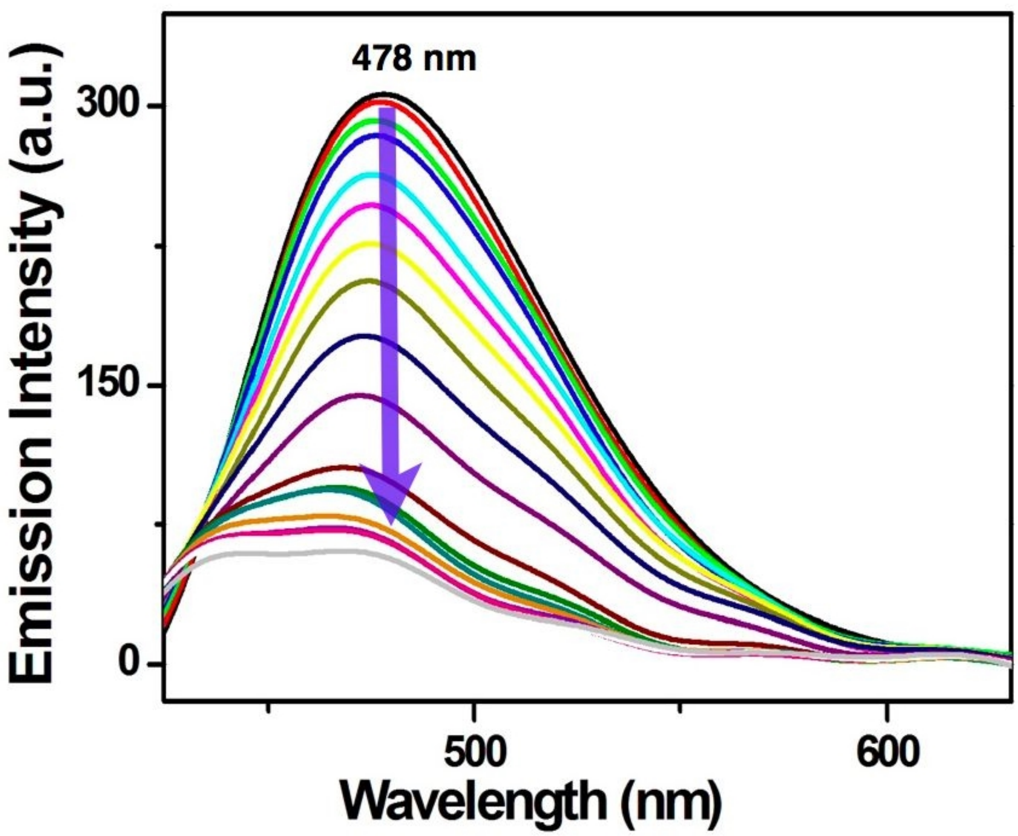

Figure S19. Fluorescence titration of **1**-Zn^{2+} complex in DMF-H_2O solvent (v/v, 7:3) upon addition of (0-5 equivalents) of EDTA.

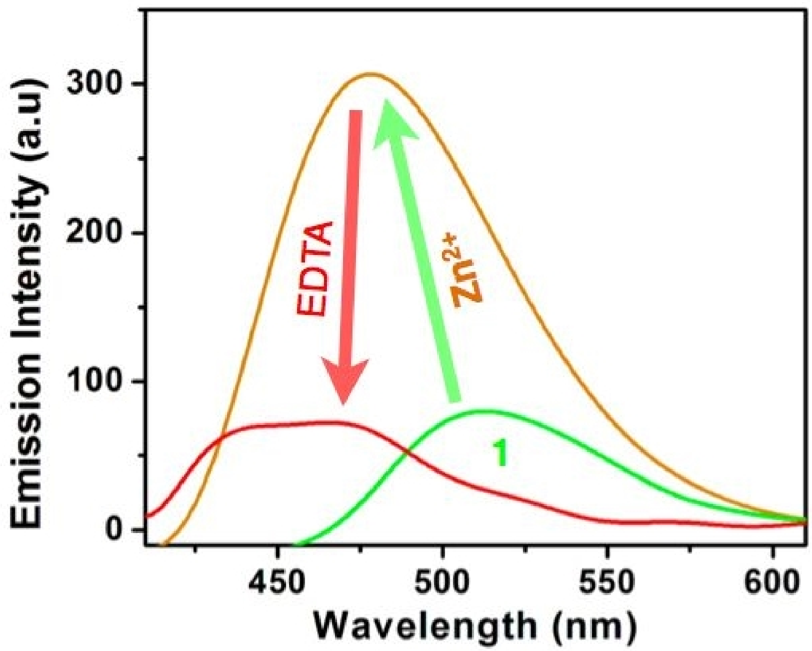

Figure S20. Fluorescence intensity change of **1** and **1**-Zn^{2+} complex upon addition of Zn^{2+} and EDTA sequentially in DMF-H_2O solvent (v/v, 7:3)

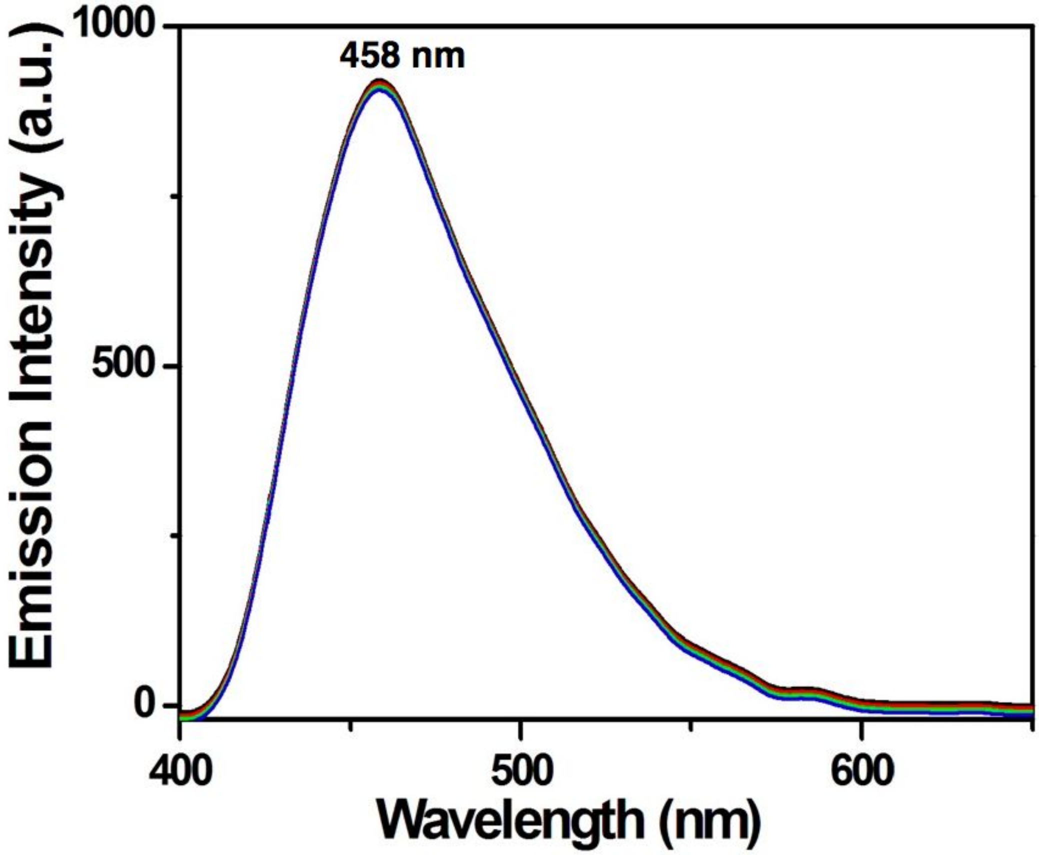

Figure S21. Fluorescence titration of **1**-Al^{3+} complex in DMF- H_2O solvent (v/v, 7:3) upon addition of (0-5 equivalents) of EDTA.

14. Comparative table:

Table S1: Comparative table of past reported probes on the basis of their medium, binding constant, limit of detection and application.

Sl.No.	Analyte	Medium	Method	Binding Constant(K_b)	Detection limit (M)	Applications	Ref.
1	Al^{3+} Cu^{2+}	EtOH/Water	Fluorometric Colorimetric	Al^{3+}: 2.83 ×10^{10} Cu^{2+}:5.69 × 10^9	Al^{3+}: 9.10 ×10^{-8} Cu^{2+}: 3.54 ×10^{-7}	Logic gate, Live cell imaging and paper strips	1
2	Al^{3+}, F^-	DMSO/ H_2O	Fluorometric	Al^{3+}:8.50 × 10^5	Al^{3+}: 1.05 ×10^{-8}	Logic gate, Live cell imaging	2
3	Al^{3+} $H_3PO_4^-$	CH_3OH	Fluorometric	Al^{3+}: 3.6 × 10^4	Al^{3+}: 8.30 × 10^{-7} $H_3PO_4^-$: 1.7×10^{-6}	Paper strips	3
4	Al^{3+} Zn^{2+}	CH_3OH/HEPES Buffer	Fluorometric	Al^{3+}: 1.3 × 10^6 Zn^{2+}: 7.9× 10^4	Al^{3+}: 8.30 × 10^{-8} Zn^{2+}: 1.24× 10^{-7}	Logic gate Live cell imaging	4
5	Al^{3+}	CH_3OH / H_2O	Fluorometric	Al^{3+}: 5.42 × 10^5	Al^{3+}: 3.55 × 10^{-7}	Paper strips Logic gate	5
6	Al^{3+} Cr^{3+}	CH_3CN	Fluorometric	Al^{3+}: 5.44 × 10^4 Cr^{3+}: 8.33 × 10^4	Al^{3+}: 3.1 × 10^{-7} Cr^{3+}: 2.5 × 10^{-7}	-	6
7	Al^{3+}	DMSO/ H_2O	Fluorometric	Al^{3+}: 4.09 × 10^4	Al^{3+}: 1.20× 10^{-7}	Live cell imaging	7
8	Al^{3+}	DMSO/ H_2O	Fluorometric		Al^{3+}: 1.90× 10^{-6}	-	8
9	Al^{3+}	CH_3OH /H_2O	Fluorometric	2.85× 10^5	Al^{3+}: 1.1× 10^{-7}	-	9
10	Al^{3+} Zn^{2+} Cd^{2+}	CH_3OH /HEPES Buffer	Fluorometric	Al^{3+}: 1.5×$10^3$$M^{-1/2}$ Zn^{2+}: 5× 10^5 Cd^{2+}: 3.5× 10^5	Al^{3+}: 5.7× 10^{-9} Zn^{2+}: 1.09× 10^{-6} Cd^{2+}: 1.64× 10^{-6}	-	10
11	Al^{3+} Cu^{2+}	CH_3CN	Fluorometric Colorimetric	Al^{3+}: 1.80× 10^4 Cu^{2+}: 2.02×10^4	Al^{3+}: 1.48× 10^{-6} Cu^{2+}: 2.05× 10^{-6}	-	11
12	Al^{3+}	DMF/H_2O	Fluorometric	Al^{3+}: 2.75× 10^3	Al^{3+}: 4.9× 10^{-7}	Paper strips	12
13	Al^{3+}	CH_3OH	Fluorometric	Al^{3+}: 1.6× 10^4	Al^{3+}: 2.7× 10^{-7}	Paper strips	13
14	Al^{3+}	DMSO	Fluorometric	Al^{3+}: 1.4× 10^4	Al^{3+}: 2.0× 10^{-7}	Paper strips	14
15	Al^{3+} Zn^{2+}	CH_3OH /H_2O Buffer CH_3OH /H_2O Buffer	Fluorometric	Al^{3+}: 1.94× 10^4 Zn^{2+}:1.19× 10^5	Al^{3+}: 1.45× 10^{-7} Zn^{2+}:1.29× 10^{-8}	-	15
16	Al^{3+} Zn^{2+}	Tris-HCl buffer EtOH /H_2O	Fluorometric	Al^{3+}: 3.50× 10^9 M^{-2} Zn^{2+}: 4.27×10^4 M^{-1}	Al^{3+}: 1.27 × 10^{-7} M Zn^{2+}: 5.5 ×10^{-8} M	Recovery in real samples	16
17	Al^{3+} Zn^{2+}	DMF/H_2O	Fluorometric	Al^{3+}: 2.43× 10^8 M^{-2} Zn^{2+}: 2.59×10^7 M^{-2}	Al^{3+}: 4.2 × 10^{-8} M Zn^{2+}: 3.4 ×10^{-8} M	Paper strips Logic gate	This work

15. Application study table:

Table S2: Determination of Al^{3+} recovery sample.

Sample	Al^{3+} added (μ mol L^{-1})	Al^{3+} found (μ mol L^{-1})	Recovery (%)	R.S.D (n=3)(%)
Tap water	0.00	0.00	-	-
	10.00	9.60	96.0	1.52
Drinking water	0.00	0.00	-	-
	10.00	9.80	98.0	0.73

Table S3: Determination of Zn^{2+} recovery sample.

Sample	Zn^{2+} added (μ mol L^{-1})	Zn^{2+} found (μ mol L^{-1})	Recovery (%)	R.S.D (n=3)(%)
Tap water	0.00	0.00	-	-
	10.00	9.33	93.3	2.46
Drinking water	0.00	0.00	-	-
	10.00	9.50	95.0	1.78

16. References:

1. P. Yadav, R. Kumar, S. Srikrishna, A. K. Pandey, L. H. Choudhury, C. Upadhyay, V. P. Singh, A reversible and efficient probe for dual mode recognition of Al^{3+} and Cu^{2+} with logic gate behaviour: Crystal structure, theoretical and in-vivo bio-imaging investigations, Spectrochimica Acta Part A, 267 (2022) 120552.
2. D. Sarkar, P. Ghosh, S. Gharami, T.K. Mondal, N. Murmu, A novel coumarin based molecular switch for the sequential detection of Al^{3+} and F^{-}: Application in lung cancer live cell imaging and construction of logic gate, Sens Actuators B Chem. 242 (2017) 338–346.
3. D. Choe, C. Kim, An acylhydrazone-based fluorescent sensor for sequential recognition of Al^{3+} and $H_2PO_4^{-}$, Materials 14 (2021) 6392.
4. H. Liu, T. Liu, J. Li, Y. Zhang, J. Li, J. Song, J. Qu, W.-Y. Wong, A simple Schiff base as dual-responsive fluorescent sensor for bioimaging recognition of Zn^{2+} and Al^{3+} in living cells, J. Mater. Chem. B, 6 (2018) 5435–5442.
5. G. Bartwal, K. Aggarwal, J.M. Khurana, An ampyrone based azo dye as pH-responsive and chemo-reversible colorimetric fluorescent probe for Al^{3+} in semi-aqueous medium: implication towards logic gate analysis, New J. Chem. 42 (2018) 2224–2231.
6. M. Tajbakhsh, G. Chalmardi, A. Bekhradnia, R. Hosseinzadeh, N. Hasani, M. Amiri, A new fluorene-based Schiff-base as fluorescent chemosensor for selective detection of Cr^{3+} and Al^{3+}, Spectrochim. Acta A, 189 (2018) 22–31.
7. A. Saravanan, S. Shyamsivappan, N. Kalagatur, T. Suresh, N. Maroli, N. Bhuvanesh, P. Kolandaivel, P. Mohan, Application of real sample analysis and biosensing: synthesis of new naphthyl derived chemosensor for detection of Al^{3+} ions, Spectrochim. Acta A, 241 (2020) 118684.
8. R. Shanmugapriya, P. Kumar, K. Poongodi, C. Nandhini, K.P. Elango, 3-Hydroxy- 2-naphthoic hydrazide as a probe for fluorescent detection of cyanide and aluminium ions in organic and aquo-organic media and its application in food and pharmaceutical samples, Spectrochim. Acta A, 249 (2021) 119315.
9. V. Kumar, S. Kundu, B. Sk, A. Patra, A naked-eye colorimetric sensor for methanol and ‘turn-on’ fluorescence detection of Al^{3+}, New J. Chem., 43 (2019) 18582–18589.

10. N. Behera, V. Manivannan, A Probe for Multi Detection of Al^{3+}, Zn^{2+} and Cd^{2+} Ions via Turn-On Fluorescence Responses, J. Photochem. Photobiol. A, 353 (2018) 77–85.

11. B. Kaura, A. Gupta, N. Kaur, A simple Schiff base as a multi responsive and sequential sensor towards Al^{3+}, F and Cu^{2+} ions, J. Photochem. Photobiol. A 389 (2020) 112140.

12. A. Mondal, E. Ahmmed, S. Chakraborty, A. Sarkar, S. Lohar, P. Chattopadhyay, Aggregation induced emission enhancement (AIEE) of naphthalene appended organic moiety: An Al^{3+} ion selective turn on fluorescent probe, Chemistry Select, 5 (2020) 147 –155.

13. G. Kumar, K. Paul, V. Luxami, Aggregation induced emission -excited state intramolecular proton transfer based “off-on” fluorescent sensor for Al^{3+} ions in liquid and solid state, Sens. Actuators B. Chem. 263 (2018) 585 –593.

14. X. Mei Jiang, W.H. Mi, W. Zhu, H. Yao, Y.M. Zhang, T.B. Wei, Q. Lin, A biacylhydrazone-based chemosensor for fluorescence ‘turn-on’ detection of Al^{3+} with high selectivity and sensitivity, Supramolecular Chemistry, 31 (2019) 80–88.

15. Y. Xu, H. Wang, J. Zhao, X. Yang, M.Pei, G. Zhang, Y. Zhang, A dual functional fluorescence sensor for detection of Al^{3+} and Zn^{2+} in different solvent, New J. Chem., 43 (2019) 14320–14326.

16. Y. Tang, J. Sun and B. Yin, A dual-response fluorescent probe for Zn^{2+} and Al*3*+ detection in aqueous media: pH-dependent selectivity and practical application *Anal. Chim. Acta*, 942 (2016), 104.